J. Plasma Phys. (2018), *vol.* 84, 905840116
doi:10.1017/S0022377818000181

Gyrokinetic stability of electron–positron–ion plasmas

A. Mishchenko[1,†], A. Zocco[1], P. Helander[1] and A. Könies[1]

[1]Max Planck Institute for Plasma Physics, D-17491 Greifswald, Germany

(Received 15 September 2017; revised 30 January 2018; accepted 31 January 2018)

The gyrokinetic stability of electron–positron plasmas contaminated by an ion (proton) admixture is studied in a slab geometry. The appropriate dispersion relation is derived and solved. Stable K-modes, the universal instability, the ion-temperature-gradient-driven instability, the electron-temperature-gradient-driven instability and the shear Alfvén wave are considered. It is found that the contaminated plasma remains stable if the contamination degree is below some threshold and that the shear Alfvén wave can be present in a contaminated plasma in cases where it is absent without ion contamination.

Key words: plasma instabilities, plasma waves

1. Introduction

The prospects for creating electron–positron pair plasmas magnetically confined in dipole or stellarator geometries have been discussed since the early 2000s (Pedersen *et al.* 2003, 2012). In the near future, the first experiment aiming at this goal will be constructed (Saitoh *et al.* 2015). It is planned to confine electron–positron plasmas in a cylindrical an approximately 20 litre vacuum vessel with a levitated coil. The electrons are to be injected with an electron gun and the positrons will be supplied from the research neutron source at the Technical University of Munich. One expects the following plasma parameters: plasma density in the range $10^{10}\ \mathrm{m}^{-3} < n < 10^{12}\ \mathrm{m}^{-3}$, temperature in the range $1\ \mathrm{eV} < T < 10\ \mathrm{eV}$, Debye length $\lambda_D = \sqrt{\epsilon_0 T/(2ne^2)} < 10^{-2}$ m and gyroradius $\rho \ll \lambda_D$. Recently, efficient injection and trapping of a cold positron beam in a dipole magnetic field configuration has been demonstrated by Saitoh *et al.* (2015). This result is a key step towards the ultimate aim of creating and studying of the first man-made magnetically confined pair plasma in the laboratory.

It has been shown by Helander (2014) that pair plasmas possess unique gyrokinetic stability properties thanks to the mass symmetry between the particle species. For example, drift instabilities are completely absent in straight unsheared geometry, e.g. in a slab. They can be destabilised only in the presence of magnetic curvature in more complicated confining fields. Helander & Connor (2016) found that this result persists also in the electromagnetic regime. However, what happens if the perfect mass symmetry between the positively charged particles (positrons) and the

† Email address for correspondence: alexey.mishchenko@ipp.mpg.de

K-modes (ion type)	Stable	Electrostatic
K-modes (electron type)	Stable	Electrostatic
Universal instability	Density gradient	Electrostatic
ITG instability	Ion temperature gradient	Electrostatic
ETG instability	Electron temperature gradient	Electrostatic
Shear Alfvén waves	Stable	Electromagnetic

TABLE 1. Gyrokinetic modes in slab geometry. The mode name appears in the first column. The second column indicates whether the mode is stable or not. For unstable modes, the destabilising gradient is written. The third column indicates if the mode requires an electromagnetic component to exist or if the electrostatic perturbation is sufficient. In pure pair plasmas, only K-modes of the electron type exist. Other modes require some degree of proton contamination.

negatively charged ones (electrons) is broken? This can happen if some fraction of ions (e.g. protons) is introduced into the pair plasma, which will probably be the case in experiments since the pumping and vacuum systems are never completely perfect. Then one could expect that the drift instabilities will reappear.

In this paper, we address the effect of proton contamination on the gyrokinetic stability of pair plasmas. We find that drift instabilities can indeed appear in contaminated pair plasmas if the proton fraction exceeds some threshold. Also, we find that the shear Alfvén wave is present in a contaminated plasma even if the ion contamination is small. Its frequency, however, increases rapidly when the ion fraction becomes negligible.

The structure of the paper is as follows. In § 2, the general electromagnetic dispersion relation is derived. It describes slab gyrokinetic stability in plasmas with an arbitrary number of species, although we consider only three species in this work. Solutions of this dispersion relation can be classified with respect to the driving gradient, stability and nature of the perturbations (electrostatic or electromagnetic). A brief summary of the modes existing in a shearless slab is given in table 1. In § 3, the stable part of the gyrokinetic spectrum (K-modes) is addressed. In §§ 4, 5 and 6, drift instabilities in three-component plasmas are considered. In § 7, the shear Alfvén wave in electron–positron–ion plasmas is described. Conclusions are summarised in § 8.

2. Dispersion relation

Following Helander (2014) and Helander & Connor (2016), we use gyrokinetic theory to analyse the linear stability of electron–positron–ion plasmas. It is convenient to write the gyrokinetic distribution function in the form:

$$f_a = f_{a0}\left(1 - \frac{e_a\phi}{T_a}\right) + g_a = f_{a0} + f_{a1}, \quad f_{a1} = -\frac{e_a\phi}{T_a} f_{a0} + g_a. \tag{2.1}$$

Here, f_{a0} is a Maxwellian, a is the species index with $a = e$ corresponding to electrons, $a = p$ to positrons and $a = i$ to the ions, e_a is the electric charge, f_{a1} is the perturbed part of the distribution function and g_a is the non-adiabatic part of f_{a1}. The linearised gyrokinetic equation in this notation is

$$\mathrm{i}v_\parallel \nabla_\parallel g_a + (\omega - \omega_{\mathrm{d}a}) g_a = \frac{e_a}{T_a} \mathrm{J}_0\left(\frac{k_\perp v_\perp}{\omega_{\mathrm{c}a}}\right) (\omega - \omega_{*a}^T)(\phi - v_\parallel A_\parallel) f_{a0} \tag{2.2}$$

https://doi.org/10.1017/S0022377818000181 Published online by Cambridge University Press

with J_0 the Bessel function, ω the complex frequency of the mode, ω_{ca} the cyclotron frequency, $k_\perp$ the perpendicular wavenumber, $v_\parallel$ and $v_\perp$ the parallel and perpendicular velocities, ϕ the perturbed electrostatic potential and $A_\parallel$ the perturbed parallel magnetic potential in the Coulomb gauge. We consider an unsheared slab geometry with the coordinates (x, y, z), a uniform magnetic field $\boldsymbol{B} = B\boldsymbol{e}_z$ pointing in the z-direction and plasma profiles which are non-uniform in the x-direction. In slab geometry, the drift frequency $\omega_{da} = 0$. Other notations used are

$$\omega_{*a}^T = \omega_{*a}\left[1 + \eta_a\left(\frac{v^2}{v_{tha}^2} - \frac{3}{2}\right)\right], \quad v = \sqrt{v_\parallel^2 + v_\perp^2}, \quad k_\perp = \sqrt{k_x^2 + k_y^2} \tag{2.3a–c}$$

$$\omega_{*a} = \frac{k_y T_a}{e_a B}\frac{\mathrm{d}\ln n_a}{\mathrm{d}x}, \quad \eta_a = \frac{\mathrm{d}\ln T_a}{\mathrm{d}\ln n_a}, \quad v_{tha} = \sqrt{\frac{2T_a}{m_a}}. \tag{2.4a–c}$$

Here, m_a is the particle mass, n_a is the ambient particle density and the sign convention is such that $\omega_{*i} \leqslant 0$, $\omega_{*p} \leqslant 0$ and $\omega_{*e} \geqslant 0$. For simplicity, we will assume $k_x = 0$ and $k_\perp = k_y$ throughout the paper. Taking the Fourier transform along the parallel coordinate, we obtain:

$$(\omega - k_\parallel v_\parallel) g_a = \frac{e_a}{T_a}\mathrm{J}_0\left(\frac{k_\perp v_\perp}{\omega_{ca}}\right)(\omega - \omega_{*a}^T)(\phi - v_\parallel A_\parallel) f_{a0}. \tag{2.5}$$

This equation is trivially solved:

$$g_a = \frac{\omega - \omega_{*a}^T}{\omega - k_\parallel v_\parallel}\frac{e_a f_{a0}}{T_a}\mathrm{J}_0(\phi - v_\parallel A_\parallel). \tag{2.6}$$

The gyrokinetic quasineutrality condition and the parallel Ampere's law are

$$\left(\sum_a \frac{n_a e_a^2}{T_a} + \epsilon_0 k_\perp^2\right)\phi = \sum_a e_a \int g_a \mathrm{J}_0 \,\mathrm{d}^3 v, \quad A_\parallel = \frac{\mu_0}{k_\perp^2}\sum_a e_a \int v_\parallel g_a \mathrm{J}_0 \,\mathrm{d}^3 v. \tag{2.7a,b}$$

Here, ϵ_0 is the electric permittivity and μ_0 is the magnetic permeability of free space. For the electromagnetic dispersion relation, it is convenient to define:

$$W_{na} = -\frac{1}{n_a v_{tha}^n}\int \frac{\omega - \omega_{*a}^T}{\omega - k_\parallel v_\parallel}\mathrm{J}_0^2 f_{a0}\, v_\parallel^n \,\mathrm{d}^3 v. \tag{2.8}$$

Taking velocity-space integrals, one finds:

$$W_{na} = \zeta_a\left\{\left(1 - \frac{\omega_{*a}}{\omega}\right) Z_{na}\Gamma_{0a} + \frac{\omega_{*a}\eta_a}{\omega}\left[\frac{3}{2}Z_{na}\Gamma_{0a} - Z_{na}\Gamma_{*a} - Z_{n+2,a}\Gamma_{0a}\right]\right\}. \tag{2.9}$$

Here, the following notation is employed:

$$\frac{1}{\lambda_{Da}^2} = \frac{e_a^2 n_a}{\epsilon_0 T_a}, \quad \frac{1}{\lambda_D^2} = \sum_a \frac{1}{\lambda_{Da}^2}, \quad b_a = k_\perp^2 \rho_a^2, \quad \rho_a = \frac{\sqrt{m_a T_a}}{|e_a| B} \tag{2.10a–d}$$

$$\Gamma_{*a} = \Gamma_{0a} - b_a[\Gamma_{0a} - \Gamma_{1a}], \quad \Gamma_{0a} = \mathrm{I}_0(b_a)\mathrm{e}^{-b_a}, \ \Gamma_{1a} = I_1(b_a)\mathrm{e}^{-b_a} \tag{2.11}$$

https://doi.org/10.1017/S0022377818000181 Published online by Cambridge University Press

$$Z_{na} = \frac{1}{\sqrt{\pi}} \int_{-\infty}^{\infty} \frac{x^n \mathrm{e}^{-x^2} \mathrm{d}x}{x - \zeta_a}, \quad \zeta_a = \frac{\omega}{k_\parallel v_{\mathrm{th}a}} \tag{2.12}$$

with I_0 and I_1 denoting the modified Bessel functions of the first kind. Using this notation, we can cast the field equations into the form:

$$(1 + k_\perp^2 \lambda_D^2)\phi + \sum_a \frac{\lambda_D^2}{\lambda_{Da}^2}(W_{0a}\phi - W_{1a} A_\parallel v_{\mathrm{th}a}) = 0 \tag{2.13}$$

$$A_\parallel + \frac{1}{c^2} \sum_a \frac{v_{\mathrm{th}a}}{k_\perp^2 \lambda_{Da}^2}(W_{1a}\phi - W_{2a} A_\parallel v_{\mathrm{th}a}) = 0. \tag{2.14}$$

Computing the determinant of this system of equations, we find the electromagnetic dispersion relation describing an electron–positron–ion plasma in a slab geometry:

$$\left(1 + k_\perp^2 \lambda_D^2 + \sum_a \frac{\lambda_D^2}{\lambda_{Da}^2} W_{0a}\right)\left(1 - 2\sum_a \frac{\beta_a}{k_\perp^2 \rho_a^2} W_{2a}\right) + 2\sum_a \frac{\lambda_D^2}{\lambda_{Da}^2} W_{1a} v_{\mathrm{th}a} \sum_a \frac{\beta_a}{k_\perp^2 \rho_a^2} \frac{W_{1a}}{v_{\mathrm{th}a}} = 0. \tag{2.15}$$

Here, $\beta_a = \mu_0 n_a T_a / B^2$. The electrostatic limit corresponds, as usual, to $\beta_a = 0$.

In the following, we will use this dispersion relation in order to describe instabilities which can appear in three-component plasmas. This will give us insight into the general properties of the gyrokinetic stability of such plasmas.

3. Gyrokinetic stable modes

We first consider the case of a pure electrostatic electron–positron plasma. Assuming quasineutrality $\omega_{*p} = -\omega_{*e}$, equal temperatures $T_p = T_e$ and equal temperature gradients $\eta_p = \eta_e$, we can reduce the dispersion relation to

$$1 + k_\perp^2 \lambda_{\mathrm{D}}^2 + \zeta Z_0 = 0 \tag{3.1}$$

with the electron and positron finite Larmor radius (FLR) effects neglected for simplicity, implying that $\Gamma_{0e} = \Gamma_{0p} = 1$. Here, we use the notation $Z_0 = Z_{0e} = Z_{0p}$ and $\zeta = \zeta_e = \zeta_p$. Equations of this type have been considered in detail by Fried & Gould (1961) and Yegorenkov & Stepanov (1987, 1988) for conventional (hydrogen) plasmas. In a hydrogen plasma, equation (3.2), similar to (3.1), describes the plasma stability in the absence of the density and temperature gradients for $T_i = T_e$:

$$1 + k_\perp^2 \lambda_{\mathrm{D}}^2 + \tfrac{1}{2}\left[\zeta_i Z_0(\zeta_i)\Gamma_{0i} + \zeta_e Z_0(\zeta_e)\Gamma_{0e}\right] = 0. \tag{3.2}$$

This equation has an infinite number of solutions, called K-modes (Yegorenkov & Stepanov 1987, 1988). These modes can be of the ion type with $\zeta_i \geqslant 1$ and $\zeta_e \ll 1$, or of the electron type with $\zeta_e \geqslant 1$. In figure 1, the spectrum resulting from (3.2) for the conventional plasma is plotted including K-modes of the ion type. This spectrum was computed numerically using the Nyquist technique (Carpentier & Santos 1982; Davies 1986). The staircase-like visual appearance of figures 1 and 2 is an artefact caused by

https://doi.org/10.1017/S0022377818000181 Published online by Cambridge University Press

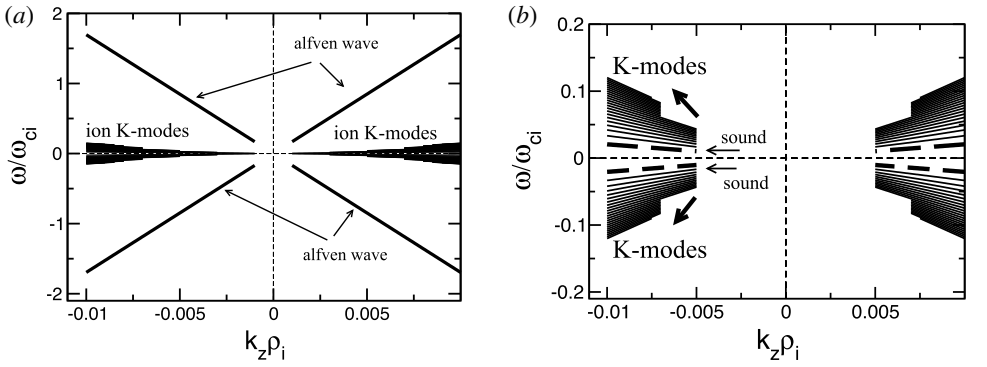

FIGURE 1. (*a*) Gyrokinetic frequency spectrum for conventional plasmas including sound wave and the electrostatic limit of the Alfvén wave. (*b*) Low-frequency part of the spectrum (K-modes of the ion type).

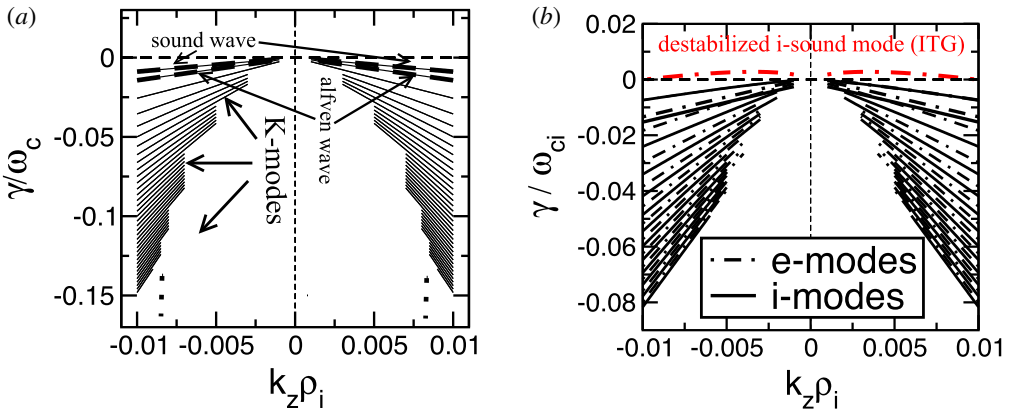

FIGURE 2. (*a*) The imaginary part of the spectrum in a homogeneous plasma. (*b*) The same in the presence of an ion temperature gradient $\kappa_{Ti}\rho_i = 0.1$ with $\kappa_{Ti} = -\mathrm{d}\ln T_i/\mathrm{d}x$. In this figure, i-modes denote modes rotating in the ion diamagnetic direction (corresponding to the negative frequencies, recall the sign convention $\omega_{*i} < 0$ and $\omega_{*e} > 0$) and e-modes correspond to modes rotating in the electron diamagnetic direction (positive frequencies).

the density of the roots of the dispersion relation increasing towards the origin of the coordinates. This complicates the numerical solution in this area.

In figure 2, one sees that, as Fried & Gould (1961) suggested, most of the solutions of (3.2) are strongly damped, satisfying $|\gamma| \sim |\omega|$. The least damped solutions can be destabilised by plasma profile gradients leading either to the ion-temperature-gradient-driven instability (ITG), the electron-temperature-gradient-driven instability (ETG) or the universal instability, driven by the density gradient. This is shown in figure 2, where the effect of the ion temperature gradient on the gyrokinetic spectrum in a conventional plasma can be seen. In pure pair plasmas, however, the electron and the positron diamagnetic contributions cancel also in presence of profile gradients, making such plasmas absolutely stable in a slab geometry within the gyrokinetic description. Note however, that perfect symmetry between the electron and positron density and temperature profiles is required to guarantee the cancellation of the

https://doi.org/10.1017/S0022377818000181 Published online by Cambridge University Press

diamagnetic terms. While density profiles are always identical for the two species in a quasineutral plasma, the temperature profiles can differ. In this case, a pure pair plasma can be temperature-gradient unstable, as we will see in the following. The gradient-driven instabilities can also appear if a pair plasma is 'contaminated' by protons or other ions.

Some analytic progress can be made for K-modes in an electron–positron plasma. Assuming $\zeta_e = \zeta_p \gg 1$ and $|\gamma| \sim |\omega|$, the plasma dispersion function can be approximated:

$$Z_0(\zeta_e) \approx 2\mathrm{i}\sqrt{\pi}\mathrm{e}^{-\zeta_e^2} - \frac{1}{\zeta_e} - \frac{1}{2\zeta_e^3}. \tag{3.3}$$

Using this expansion and neglecting the Debye length, $k_\perp \lambda_D \ll 1$, we obtain:

$$4\mathrm{i}\sqrt{\pi}\zeta_e^3\mathrm{e}^{-\zeta_e^2} = 1. \tag{3.4}$$

Introducing the notation $\zeta_e = x - \mathrm{i}y$ and assuming $x = \pm(y + \Delta)$ with $\Delta \ll y$ (Yegorenkov & Stepanov 1987, 1988), we can write the dispersion relation in the form:

$$8y^3\sqrt{2\pi}\mathrm{e}^{-2y\Delta}\exp(2\mathrm{i}y^2 - \mathrm{i}\pi/4) = 1 \equiv \exp(2\pi m\mathrm{i}). \tag{3.5}$$

Splitting this relation into equations for the argument and for the absolute value and employing $\Delta/y \ll 1$, we obtain:

$$2y^2 - \pi/4 = 2\pi m, \quad 8y^3\sqrt{2\pi}\mathrm{e}^{-2y\Delta} = 1. \tag{3.6a,b}$$

Thus, an infinite family of solutions is found:

$$y_m = \sqrt{\pi m + \pi/8} \approx \sqrt{\pi m}, \quad \Delta_m = \frac{\ln(8y_m^3\sqrt{2\pi})}{2y_m}, \quad x_m = \pm(y_m + \Delta_m). \tag{3.7a–c}$$

Finally, we write our solutions in the form:

$$\omega_m = \pm k_\parallel v_{\mathrm{the}} x_m, \quad \gamma_m = -k_\parallel v_{\mathrm{the}} y_m. \tag{3.8a,b}$$

These relations describe strongly damped K-modes in a pure electron–positron plasma. In figure 3, we compare these analytic results with the numerical solution of the original dispersion relation (2.15) and find very good agreement. Note that the expansion (3.3) is valid for $m \gg 1$. For low m, the dispersion relation must be solved numerically.

In a conventional hydrogen plasma, one can make the usual assumption $\zeta_i \gg 1$ and $\zeta_e \ll 1$ corresponding to the K-modes of the ion type. In this case, the following expansions of the plasma dispersion function can be used:

$$Z_0(\zeta_i) = 2\mathrm{i}\sqrt{\pi}\mathrm{e}^{-\zeta_i^2} - \frac{1}{\zeta_i} - \frac{1}{2\zeta_i^3}, \quad Z_0(\zeta_e) = \mathrm{i}\sqrt{\pi} - 2\zeta_e, \tag{3.9a,b}$$

which lead to the approximated dispersion relation (assuming $k_\perp \lambda_D \ll 1$):

$$(1 - \Gamma_{0i}/2) + \left(\mathrm{i}\zeta_i\sqrt{\pi}\mathrm{e}^{-\zeta_i^2} - \frac{1}{4\zeta_i^2}\right)\Gamma_{0i} + O(\zeta_e) = 0. \tag{3.10}$$

https://doi.org/10.1017/S0022377818000181 Published online by Cambridge University Press

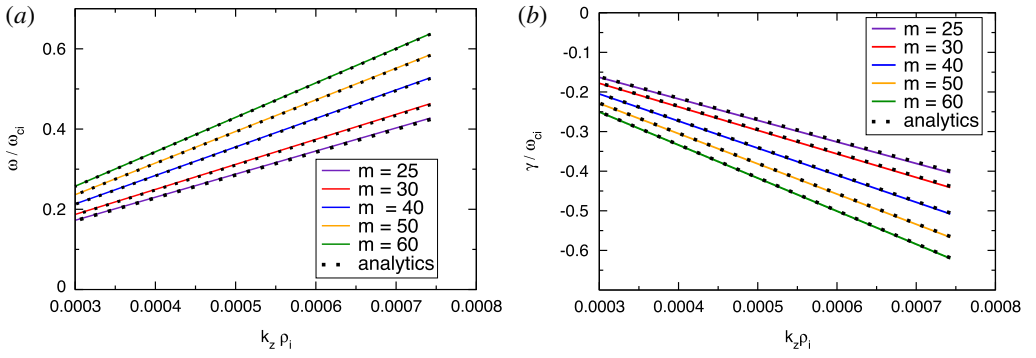

FIGURE 3. 'K-mode' solution of the dispersion relation for a pure pair plasma. All modes are strongly damped. Here, $k_\perp \lambda_D = 0$ has been assumed. The numerical solution of (2.15) is compared with the analytic result (3.8).

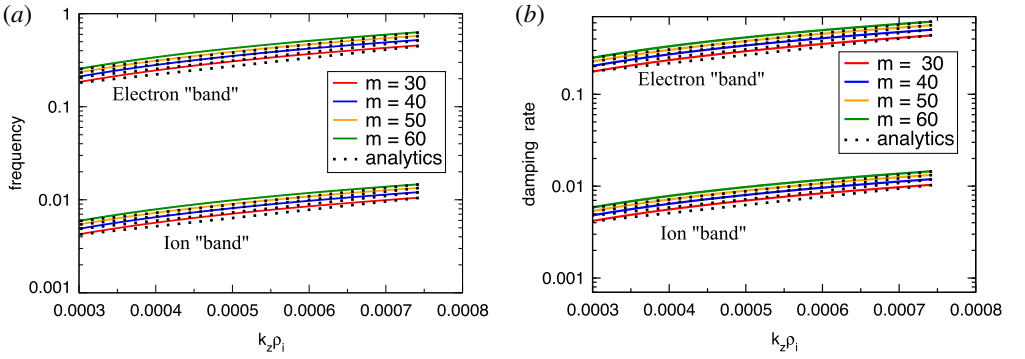

FIGURE 4. 'K-mode' solution of the dispersion relation for conventional plasma assuming $k_\perp \lambda_D = 0$. One can see the ion and the electron parts of the spectrum. The numerical solution of (2.15) is compared with the analytic result (3.13). For the numerical solution, we set the density and temperature gradients appearing in (2.15) to zero.

For simplicity, we neglect FLR effects, implying $\Gamma_{0i} = 1$. Also, the small contribution $1/(4\zeta_i^2) \ll 1$ can be neglected compared to the other terms. Then, we obtain:

$$2\mathrm{i}\zeta_i \sqrt{\pi} \mathrm{e}^{-\zeta_i^2} + 1 = 0. \tag{3.11}$$

Using the notation $\zeta_i = x - \mathrm{i}y$ with $x = \pm(y + \Delta)$ and employing $\Delta \ll 1$, we can split the dispersion relation into equations for the argument and for the absolute value:

$$2y\sqrt{2\pi}\mathrm{e}^{-2y\Delta} \exp(2\mathrm{i}y^2 - 3\pi\mathrm{i}/4) = 1 \equiv \exp(2\pi m\mathrm{i}). \tag{3.12}$$

Finally, the solutions for the K-modes of the ion type are

$$y_m = \sqrt{\pi m + \frac{3\pi}{8}} \approx \sqrt{\pi m}, \quad \Delta_m = \frac{\ln(2y\sqrt{2\pi})}{2y}, \quad x_m = \pm(y_m + \Delta_m). \tag{3.13a,b}$$

In figure 4, these analytic results are compared with the numerical solution of the original (exact) dispersion relation (2.15).

https://doi.org/10.1017/S0022377818000181 Published online by Cambridge University Press

Interestingly, the same dispersion relation can be obtained for K-modes in a pure pair plasma keeping the Debye length finite. In this case, the dispersion relation (3.4) is replaced by

$$4\mathrm{i}\sqrt{\pi}\zeta_e^3\mathrm{e}^{-\zeta_e^2}+2\zeta_e^2k_\perp^2\lambda_D^2=1 \quad\Longrightarrow\quad 2\mathrm{i}\sqrt{\pi}\zeta_e\mathrm{e}^{-\zeta_e^2}+k_\perp^2\lambda_D^2=0, \tag{3.14}$$

which reduces to (3.11) if $k_\perp\lambda_D\gg 1/\zeta_e$ with $k_\perp\lambda_D$ replacing 1 and ζ_e replacing ζ_i.

Going back to a hydrogen plasma, we consider a regime with $\zeta_i\gg\zeta_e\gg 1$ corresponding to the K-modes of the electron type. In this case, we can expand

$$Z_0(\zeta_i)=2\mathrm{i}\sqrt{\pi}\mathrm{e}^{-\zeta_i^2}-\frac{1}{\zeta_i}-\frac{1}{2\zeta_i^3},\quad Z_0(\zeta_e)=2\mathrm{i}\sqrt{\pi}\mathrm{e}^{-\zeta_e^2}-\frac{1}{\zeta_e}-\frac{1}{2\zeta_e^3}. \tag{3.15a,b}$$

A dispersion relation very similar to that describing the K-modes of the ion type, see (3.11), can be derived for the K-modes of the electron type keeping ion FLR terms and neglecting the electron FLR effects. This can be done since $\rho_e\ll\rho_i$; it implies $\Gamma_{0e}\approx 1$. In this case, we obtain:

$$\frac{1-\Gamma_{0i}}{2}+\left(\mathrm{i}\zeta_e\sqrt{\pi}\mathrm{e}^{-\zeta_e^2}-\frac{1}{4\zeta_e^2}\right)+O\left(\frac{1}{\zeta_i^2}\right)=0. \tag{3.16}$$

Here, recall that $\zeta_i\gg\zeta_e$. At finite $k_\perp\rho_i\gg 1/\zeta_e$, implying $1-\Gamma_{0i}\gg 1/\zeta_e^2$, one can neglect the last term in (3.16), transforming it to

$$2\mathrm{i}\zeta_e\sqrt{\pi}e^{-\zeta_e^2}+(1-\Gamma_{0i})=0. \tag{3.17}$$

This equation and, hence, its solution coincide with the dispersion relation (3.11) for the K-modes of the ion type if we replace the last term in (3.11) with $(1-\Gamma_{0i})$ and ζ_i with ζ_e. In the opposite limit of negligible $k_\perp\rho_i\ll 1/\zeta_e$, the dispersion relation for the K-modes of the electron type, equation (3.16), becomes

$$\mathrm{i}\zeta_e\sqrt{\pi}\mathrm{e}^{-\zeta_e^2}-\frac{1}{4\zeta_e^2}=0 \quad\Longleftrightarrow\quad 4\mathrm{i}\zeta_e^3\sqrt{\pi}\mathrm{e}^{-\zeta_e^2}=1. \tag{3.18}$$

This equation and its solution coincide exactly with the pair-plasma K-mode dispersion relation with $k_\perp\lambda_D$ neglected, see (3.4).

In a three-component plasma with the ion fraction $\nu_i=n_i/n_e$, the K-mode dispersion relation for $\zeta_e\gg 1$ (electron type) becomes

$$\nu_i(1-\Gamma_{0i})+(2-\nu_i)\left(2\mathrm{i}\zeta_e\sqrt{\pi}\mathrm{e}^{-\zeta_e^2}-\frac{1}{2\zeta_e^2}\right)+O\left(\frac{1}{\zeta_i^2}\right)=0. \tag{3.19}$$

The last term ($\sim 1/\zeta_e^2$) is negligible unless $\nu_i\to 0$ or $k_\perp\to 0$. Here, electron and positron FLR effects have been neglected.

In summary, K-modes, considered in this section, are the only solutions of the slab dispersion relation in pure electron–positron plasma for arbitrary density and temperature profiles provided these profiles coincide for the two species. If the positron and the electron temperature profiles differ, a temperature-driven instability can appear also for pure pair plasma in a slab geometry. This will be considered in more detail in the following.

https://doi.org/10.1017/S0022377818000181 Published online by Cambridge University Press

4. Universal instability

The first unstable mode to be considered is the universal instability driven by the density gradient. For simplicity, we assume the temperature profiles to be flat and equal, i.e. $T_i = T_e = T_p$. In this case, the dispersion relation is

$$1 + k_\perp^2 \lambda_D^2 + \frac{1}{2} \sum_{a=i,p,e} \nu_a \zeta_a \left(1 - \frac{\omega_{*a}}{\omega}\right) Z_{0a} \Gamma_{0a} = 0. \tag{4.1}$$

Here, $\nu_a = n_a/n_e$ is the density fraction corresponding to a particular species $a = i, e, p$. For electrons, $\nu_e = 1$. Taking the limit $k_\parallel v_{\mathrm{th}i} \ll \omega \ll k_\parallel v_{\mathrm{th}e}$, we obtain:

$$Z_{0i} \approx -\frac{1}{\zeta_i}, \quad Z_{0e} \approx \mathrm{i}\sqrt{\pi}. \tag{4.2a,b}$$

Let us introduce the notation $\omega_* = -\omega_{*i}$. Employing the quasineutrality, $\nu_e = \nu_p + \nu_i$ and $\nu_i \omega_{*i} + \nu_e \omega_{*e} + \nu_p \omega_{*p} = 0$, we obtain to lowest order:

$$\left[2\left(1 + k_\perp^2 \lambda_D^2\right) - \nu_i \Gamma_{0i}\right] \omega - \nu_i \omega_* \Gamma_{0i} + \mathrm{i}\zeta_e \sqrt{\pi} [\omega(\nu_e + \nu_p) - \nu_i \omega_*] = 0. \tag{4.3}$$

Here, the electron and positron FLR have been neglected $\Gamma_{0e} = \Gamma_{0p} = 1$. We solve the dispersion relation for $\omega = \omega_r + \mathrm{i}\,\gamma$ assuming $\omega_r \gg \gamma$. Then, to the lowest order,

$$\omega_r = \frac{\nu_i \omega_* \Gamma_{0i}}{2\left(1 + k_\perp^2 \lambda_D^2\right) - \nu_i \Gamma_{0i}}, \quad \gamma = \frac{2\omega_r}{k_\parallel v_{\mathrm{th}e}} \sqrt{\pi}\, \nu_i \omega_* \frac{k_\perp^2 \lambda_D^2 + (1 - \Gamma_{0i})}{\left[2\left(1 + k_\perp^2 \lambda_D^2\right) - \nu_i \Gamma_{0i}\right]^2}. \tag{4.4a,b}$$

One sees that in the long-wavelength limit, $\Gamma_{0i} \to 1$, the universal mode is unstable for finite $k_\perp \lambda_D$ with ω_r independent of λ_D and γ proportional to $k_\perp^2 \lambda_D^2$ for small $k_\perp^2 \lambda_D^2$. For large $k_\perp^2 \lambda_D^2$, both ω_r and γ are proportional to $1/k_\perp^2 \lambda_D^2$. This behaviour is seen in the numerical solution of the dispersion relation (2.15) shown in figure 5. Here, we use the parameters $k_\perp \rho_i = 0.1$, $k_\parallel \rho_i = 7.43 \times 10^{-4}$, $\kappa_{ni}\rho_i = \kappa_{ne}\rho_i = \kappa_{np}\rho_i = 0.3$ and $\kappa_{Ti}\rho_i = \kappa_{Te}\rho_i = \kappa_{Tp}\rho_i = 0.0$ with $\kappa_{na} = -\mathrm{d}\ln n_a/\mathrm{d}x$ and $\kappa_{Ta} = -\mathrm{d}\ln T_a/\mathrm{d}x$. For these parameters, $\omega_*/\omega_{\mathrm{ci}} = k_y \kappa_{ni} \rho_i^2 = 0.03$. Recall that x denotes the direction of non-uniformity of the plasma profiles, see § 2.

From (4.4) one sees that to be unstable at $\lambda_D = 0$, the universal mode needs a finite and large enough value of $1 - \Gamma_{0i}$, which is the case if $k_\perp \rho_i \sim 1$. The numerical solution corresponding to this case is shown in figure 6. The dispersion relation (2.15) is solved for the parameters $k_\perp \rho_i = 2.0$, $k_\parallel \rho_i = 7.4 \times 10^{-4}$, $\kappa_{Ti} = \kappa_{Te} = 0$, $\lambda_D = 0$. One sees that the universal instability can exist in pair plasmas in a slab geometry but requires both the proton fraction and the ion density gradient to exceed some threshold. Note that one would have to include resonant contributions (e.g. proportional to $\mathrm{e}^{-\zeta_i^2}$) and other higher-order terms into the growth rate calculation to find the threshold analytically. Such terms have been omitted in the derivation of (4.4), which is therefore valid only in the unstable domain. It is however straightforward to find the threshold numerically. Practically, it suggests that the universal mode will be stable in pair plasmas if the proton contamination is small. Interestingly, the positron density gradient has zero effect on the universal mode if quasineutrality $n_e = n_p + n_i$ is assumed since any effect of the positron density gradient on the universal mode is perfectly cancelled by the electrons. Note, however, that the positrons still contribute through their finite fraction since $\nu_i = 1 - \nu_p$.

https://doi.org/10.1017/S0022377818000181 Published online by Cambridge University Press

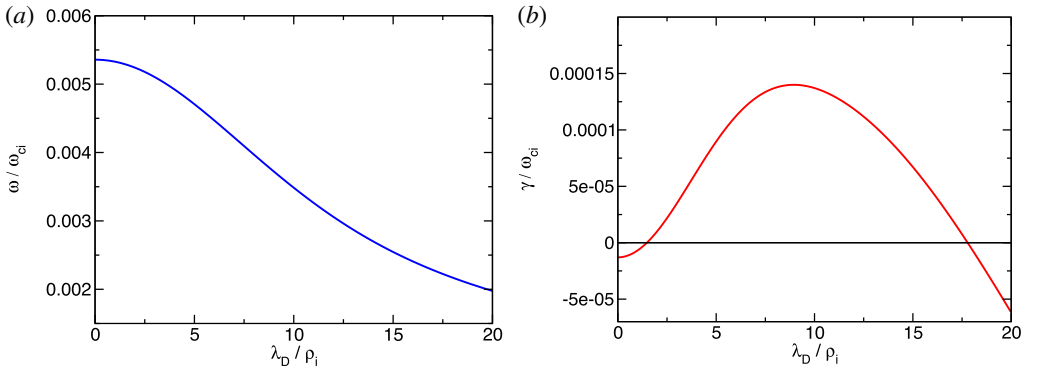

FIGURE 5. Frequency and growth rate of the universal mode as functions of the Debye length in a contaminated pair plasma with the positron fraction $\nu_p = 0.7$. The parameters are $k_\perp \rho_i = 0.1$, $k_\parallel \rho_i = 7.43 \times 10^{-4}$, $\kappa_{ni}\rho_i = \kappa_{ne}\rho_i = \kappa_{np}\rho_i = 0.3$, and $\kappa_{Ti}\rho_i = \kappa_{Te}\rho_i = \kappa_{Tp}\rho_i = 0.0$ with $\kappa_{na} = -\mathrm{d}\ln n_a/\mathrm{d}x$ and $\kappa_{Ta} = -\mathrm{d}\ln T_a/\mathrm{d}x$. For these parameters, $\omega_*/\omega_{ci} = k_y \kappa_{ni}\rho_i^2 = 0.03$.

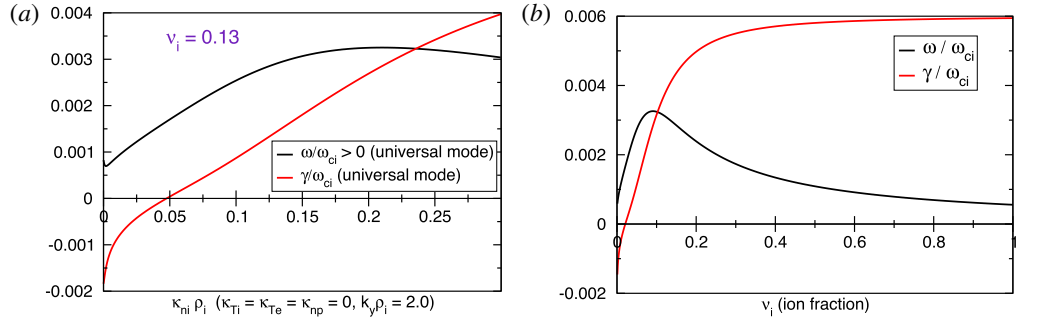

FIGURE 6. Frequency and growth rate of the universal mode in a contaminated pair plasma. One sees that the ion density gradient and the ion contamination must be larger than some threshold for the mode to become unstable. The ion density gradient $\kappa_{ni}\rho_i = 0.3$ has been used for the ν_i dependence (*b*).

5. ITG instability

For simplicity, we consider the flat density limit for all species. In this case, it is convenient to define $\omega_{Ta} = \eta_a \omega_{*a} = k_y T_a/(e_a B)\,\mathrm{d}\ln T_a/\mathrm{d}x$, which is finite also at zero density gradient, with $a = i, e, p$ being the species index. For electrons and positrons, we also assume flat temperature profiles $\omega_{Te} = \omega_{Tp} = 0$. Only for ions is the temperature gradient finite, $\omega_{Ti} \neq 0$. To allow for unequal temperatures of different species, we introduce the notation:

$$\hat{\nu}_a = \frac{2\,\nu_a/\tau_a}{\sum_{a'} \nu_{a'}/\tau_{a'}} \tag{5.1}$$

with $\nu_a = n_a/n_e$ and $\tau_a = T_a/T_e$. Note that quasineutral plasmas satisfy both $\sum_a \nu_a = 2$ and $\sum_a \hat{\nu}_a = 2$. If the temperatures of all species are equal ($\tau_a = 1$) in such plasmas, then $\hat{\nu}_a = \nu_a$. Using this notation and assuming, as already mentioned, flat density

https://doi.org/10.1017/S0022377818000181 Published online by Cambridge University Press

profiles for all species ($\omega_{*a}=0$), the dispersion relation becomes

$$1+k_\perp^2\lambda_D^2+\sum_{a=i,p,e}\frac{\hat{\nu}_a}{2}\zeta_a Z_{0a}\Gamma_{0a}+\frac{\hat{\nu}_i\omega_{Ti}\,\zeta_i}{2\omega}\left(\frac{3}{2}Z_{0i}\Gamma_{0i}-Z_{0i}\Gamma_{*i}-Z_{2i}\Gamma_{0i}\right)=0. \tag{5.2}$$

We consider the long-wavelength limit $\Gamma_{0a}=\Gamma_{*a}=1$ for all particle species. For the ITG instability, we can assume $k_\parallel v_{\mathrm{th}i}\ll\omega\ll k_\parallel v_{\mathrm{th}e}$. Then, the plasma dispersion function can be expanded as

$$Z_0(\zeta_i)\approx-\frac{1}{\zeta_i}-\frac{1}{2\zeta_i^3}-\frac{3}{4\zeta_i^5},\quad Z_0(\zeta_p)=Z_0(\zeta_e)\approx \mathrm{i}\sqrt{\pi}. \tag{5.3a,b}$$

Using (2.12), it is straightforward to derive $Z_{2i}=\zeta_i(1+\zeta_i Z_{0i})$. Here, one sees that the fifth-order term must be included into the expansion of Z_{0i} appearing in Z_{2i} since we need cubic ($\sim 1/\zeta_i^3$) terms for the ITG instability and we must keep all of them for consistency. Neglecting ion FLR effects (i.e. setting $\Gamma_{0i}=1$ and $\Gamma_{*i}=1$) as well as the electron and positron contributions ($\sim\zeta_e\ll 1$), we obtain to leading order in $1/\zeta_i$

$$1-\frac{\hat{\nu}_i}{2}+k_\perp^2\lambda_D^2=-\frac{\hat{\nu}_i\omega_{Ti}}{4\omega\zeta_i^2}+\frac{\nu_i}{2\zeta_i^2}. \tag{5.4}$$

Following Coppi, Rosenbluth & Sagdeev (1967), we also assume $\omega_{Ti}\gg\omega$. Then

$$1-\frac{\hat{\nu}_i}{2}+k_\perp^2\lambda_D^2=-\frac{\hat{\nu}_i\omega_{Ti}}{4\omega^3}k_\parallel^2 v_{\mathrm{th}i}^2. \tag{5.5}$$

Note that by definition $\omega_{Ti}=\eta_i\omega_{*i}$ with $\omega_{*i}<0$, see § 2, and $\eta_i>0$. Hence, $\omega_{Ti}<0$ and there is an unstable solution of the dispersion relation (5.5):

$$\omega=\frac{1}{2^{1/3}}\left(\frac{\hat{\nu}_i|\omega_{Ti}|k_\parallel^2 v_{\mathrm{th}i}^2}{2-\hat{\nu}_i+2k_\perp^2\lambda_D^2}\right)^{1/3}\left(-\frac{1}{2}+\mathrm{i}\frac{\sqrt{3}}{2}\right). \tag{5.6}$$

This root corresponds to the well-known fluid limit of the slab ITG instability (Coppi *et al.* 1967). Note that the real part of the ITG frequency is negative, as expected. One sees that in an ion-contaminated electron–positron plasma, the frequency and growth rate of the fluid ITG instability are proportional to $(\hat{\nu}_i|\omega_{Ti}|)^{1/3}$. Hence, pure pair plasmas with $\hat{\nu}_i=0$ cannot support the slab ITG. This is an obvious conclusion since the absence of ions guarantees the absence of ion-temperature-gradient-driven instabilities. More important, however, is that, similarly to the frequency and the growth rate, the destabilisation threshold is also determined by the product $\hat{\nu}_i|\omega_{Ti}|$, and not just $|\omega_{Ti}|$ as is the case for conventional (e.g. hydrogen) plasmas. This can be deduced from the fact that ω_{Ti} appears only in combination with ν_i in the original dispersion relation, equation (5.2). Note that the solution equation (5.6) corresponds to the fluid instability and does not contain information about the threshold. In this paper, we do not derive the threshold analytically, but we can easily find it numerically. Numerical results demonstrating this prediction are shown in figure 7. Here, the dependence of the ITG frequency and the growth rate on the proton contamination is plotted. One sees that the absolute value of the frequency indeed decreases strongly at a smaller proton content, in agreement with the analytic result. One also sees that the mode is unstable only when the proton content exceeds some

https://doi.org/10.1017/S0022377818000181 Published online by Cambridge University Press

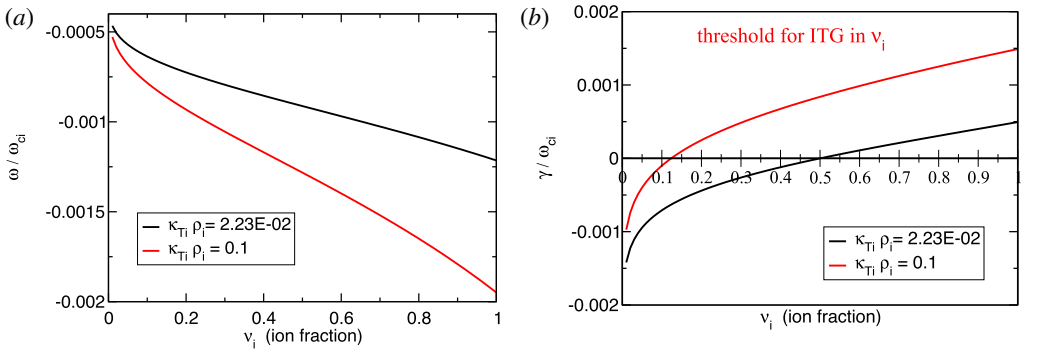

FIGURE 7. Effect of proton contamination on the ITG mode in a pair plasma. The wavenumbers are $k_\perp \rho_i = 0.24$ and $k_\parallel \rho_i = 7.4 \times 10^{-4}$. The density and the electron temperature profiles are flat, $\kappa_{Ti} = -\mathrm{d} \ln T_i(x)/\mathrm{d}x$, and $\tau_i = 1$.

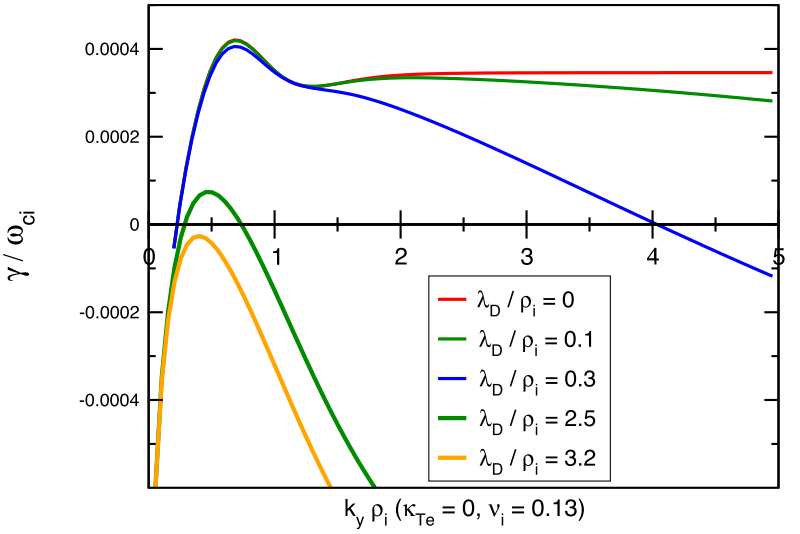

FIGURE 8. ITG mode in a pair plasma with the proton contamination $\nu_i = 0.13$ for $\tau_i = 1$ and $k_\parallel \rho_i = 7.4 \times 10^{-4}$. Effect of the finite Debye length is considered.

threshold, whose value depends on the ion temperature gradient. This is of practical interest since it indicates that the ITG modes may be stable at a large ion temperature gradient in ion-contaminated pair plasmas if the ion fraction is small enough. Other parameters, such as the density gradient or wavenumbers, can affect the value of the threshold, too, but we keep all other parameters fixed in the calculation shown in figure 7, changing only the proton fraction for two different values of the ion temperature gradient.

Another aspect of practical interest for the pair-plasma experiment (Pedersen *et al.* 2012) is the effect of the Debye length on the microinstabilities. This effect is usually negligible for tokamak or stellarator plasmas, where the Debye length is much smaller than the ion gyroradius. In the pair-plasma experiment, however, the Debye length is not expected to be very small and can become comparable to the proton gyroradius. This can have a strongly stabilising effect on the ITG stability, as shown in figure 8.

https://doi.org/10.1017/S0022377818000181 Published online by Cambridge University Press

One sees that for a given $k_\parallel$, the ITG instability can disappear for all perpendicular wavelengths if λ_D/ρ_i is large enough.

6. ETG instability

Consider now the case when only electron and positron temperature gradients are present, i.e. $\omega_{T(e,p)} \neq 0$, while $\omega_{Ti} = 0$ and $\omega_{*(e,p,i)} = 0$ (flat density). Recall that $\omega_{Ta} = k_y T_a/(e_a B)\, \mathrm{d}\ln T_a/\mathrm{d}x$ is proportional to the temperature gradient and can be finite also at $\omega_{*a} = 0$. In this section, we will also allow for unequal temperatures of different species. Therefore, the notation defined in (5.1) will be used. For the perpendicular wavenumbers, we assume $k_\perp \rho_i \gg 1$ implying $\Gamma_{0i} = 0$ and $\Gamma_{*i} = 0$. In this limit, the dispersion relation is

$$1 + k_\perp^2 \lambda_D^2 + \sum_{a=p,e} \frac{\hat{\nu}_a}{2} \zeta_a \left[Z_{0a}\Gamma_{0a} + \frac{\omega_{Ta}}{\omega} \left(\frac{3}{2} Z_{0a}\Gamma_{0a} - Z_{0a}\Gamma_{*a} - Z_{2a}\Gamma_{0a} \right) \right] = 0. \tag{6.1}$$

Here, recall that from (2.12) one can derive $Z_{2a} = \zeta_a(1 + \zeta_a Z_{0a})$. Assuming large frequencies $\omega \gg k_\parallel v_{\mathrm{th}(e,p)}$, we can write

$$Z_0(\zeta_{e,p}) \approx -\frac{1}{\zeta_{e,p}} - \frac{1}{2\zeta_{e,p}^3} - \frac{3}{4\zeta_{e,p}^5}. \tag{6.2}$$

The fifth-order term in this expansion is needed to account for the quadratic ($\sim\zeta_a^2$) contribution appearing in Z_{2a}. Assuming in addition small $k_\perp \rho_{(e,p)} \ll 1$, i.e. $\Gamma_{0(e,p)} = 1$ and $\Gamma_{*(e,p)} = 1$, we finally obtain to the leading order

$$\left(\frac{\hat{\nu}_i}{2} + k_\perp^2 \lambda_D^2 \right) + \frac{\hat{\nu}_e \tau_e \omega_{Te} + \hat{\nu}_p \tau_p \omega_{Tp}}{4\omega\zeta_e^2} = 0. \tag{6.3}$$

Here, the relations $\sum_a \hat{\nu}_a = 2$ and $\zeta_p^2 = \zeta_e^2/\tau_p$ have been employed. Similarly to the ITG derivation, equation (5.5), we have assumed $\omega_{Te} \sim \omega_{Tp} \gg \omega$, following Coppi *et al.* (1967), i.e. our derivation of (6.3) follows exactly the same path as in the ITG case, equation (5.5).

Let us now consider the case of equal electron and positron temperature profiles, implying $\tau_p = \tau_e = 1$ and $\omega_{Te} + \omega_{Tp} = 0$. Recall that $\tau_a = T_a/T_e$, and our sign conventions imply $\omega_{Te} > 0$ and $\omega_{Tp} < 0$. These conditions are likely since the characteristic time of the energy exchange between the electrons and the positrons is comparable to their Maxwellisation time. If the plasma has had time to reach a locally Maxwellian state, as we have assumed, the electron and positron temperatures should also have equilibrated. In contrast, the ion temperature can differ from the electron one, implying $\tau_i \neq 1$. Then, the unstable solution is

$$\omega = \frac{1}{2^{1/3}} \left(\frac{k_\parallel^2 v_{\mathrm{th}e}^2}{\hat{\nu}_i + 2k_\perp^2 \lambda_D^2}\, \hat{\nu}_i \tau_i \omega_{Te} \right)^{1/3} \left(\frac{1}{2} + \mathrm{i}\, \frac{\sqrt{3}}{2} \right). \tag{6.4}$$

This solution corresponds to the fluid limit of the slab ETG instability, which is similar to the ITG instability, equation (5.6), but has a frequency of the opposite sign. The mode is expected to be stable in a pure pair plasma $\hat{\nu}_i = 0$, as can indeed be seen from the numerical solution of the full dispersion relation (2.15), shown in

https://doi.org/10.1017/S0022377818000181 Published online by Cambridge University Press

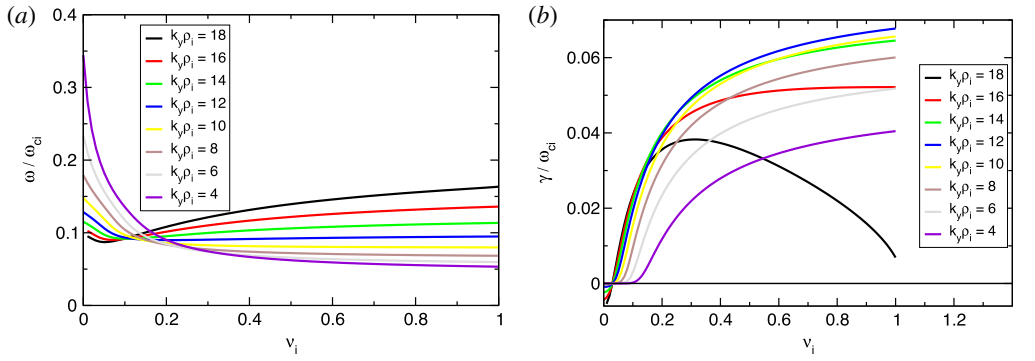

FIGURE 9. Frequency and growth rate of the ETG mode in a three-component electron–positron-proton plasma for $\omega_{Tp} = \omega_{Te}$. One sees that the ion fraction must exceed some threshold for the ETG to be unstable. Here, $k_\parallel \rho_i = 7.4 \times 10^{-4}$, $\kappa_{ni} = \kappa_{ne} = \kappa_{np} = 0$, $\kappa_{Ti} = 0$, $\kappa_{Te}\rho_i = \kappa_{Tp}\rho_i = 0.1$, $\lambda_D = 0$ and $\tau_a = 1$ with $a = (i, e, p)$.

figure 9. In (6.4), however, also the denominator vanishes at $\hat{\nu}_i = 0$ if $k_\perp \lambda_D = 0$. This singular limit contradicts to the assumption $\omega \ll \omega_{Te}$ made in the derivation of (6.4). Therefore this equation cannot be used at very small ν_i unless $k_\perp \lambda_D$ is finite. For finite $k_\perp \lambda_D$, there is no singularity and (6.4) is valid even at very small ν_i. For this regime, however, the finite Debye length effects are important. For example, ω is proportional to $(k_\perp \lambda_D)^{-2/3}$ if $\nu_i \ll k_\perp^2 \lambda_D^2$.

Now, we consider a situation in which the electron and the positron temperature gradients are different for some reason, implying $\omega_{Te} + \omega_{Tp} \neq 0$. In this case, one can show that the ETG mode can be unstable also in a pure pair plasma ($\hat{\nu}_i = 0$). Assuming for simplicity $k_\perp \lambda_D$ to be finite, we can write the unstable ETG solution as

$$\omega = \frac{1}{2^{1/3}} \left(\frac{k_\parallel^2 v_{the}^2}{k_\perp^2 \lambda_D^2} \frac{\tau_e \tau_p}{\tau_e + \tau_p} [|\omega_{Te}| - |\omega_{Tp}|] \right)^{1/3} \left(\frac{1}{2} + \mathrm{i} \frac{\sqrt{3}}{2} \right). \tag{6.5}$$

The numerical solution of the dispersion relation (2.15) corresponding to a pure pair-plasma ETG is shown in figure 10. This result is valid if the electrons have a steeper temperature profile. Otherwise, the ETG instability is replaced by the positron-temperature-gradient (PTG) driven instability, which has a negative frequency:

$$\omega = \frac{1}{2^{1/3}} \left(\frac{k_\parallel^2 v_{the}^2}{k_\perp^2 \lambda_D^2} \frac{\tau_e \tau_p}{\tau_e + \tau_p} [|\omega_{Tp}| - |\omega_{Te}|] \right)^{1/3} \left(-\frac{1}{2} + \mathrm{i} \frac{\sqrt{3}}{2} \right). \tag{6.6}$$

The PTG solution is shown in figure 11. One can see that the frequency of the PTG instability is negative whereas the frequency of the ETG instability, figure 10, is positive, as suggested by (6.5) and (6.6). The growth rates of both instabilities are equal. The absolute values of the ETG and PTG frequencies are equal, too, in agreement with (6.5) and (6.6). Finally, one can see that the growth rate increases with $|\omega_{Te} + \omega_{Tp}|$ for both instabilities. The modes are stable when $|\omega_{Te} + \omega_{Tp}| = 0$, as expected. Note that $\omega_{Te}/\omega_{ci} = k_y \kappa_{Te} \rho_i^2$ and $\omega_{Tp}/\omega_{ci} = -k_y \kappa_{Tp} \rho_i^2$, so that $\omega_{Te} + \omega_{Tp}$ is proportional to $\kappa_{Te} - \kappa_{Tp}$. Here, the ion gyroradius $\rho_i = \sqrt{m_H T_e}/(eB)$ with m_H the proton mass is defined through the electron temperature and used as a normalisation constant in pure pair plasma, which does not contain ions by definition.

https://doi.org/10.1017/S0022377818000181 Published online by Cambridge University Press

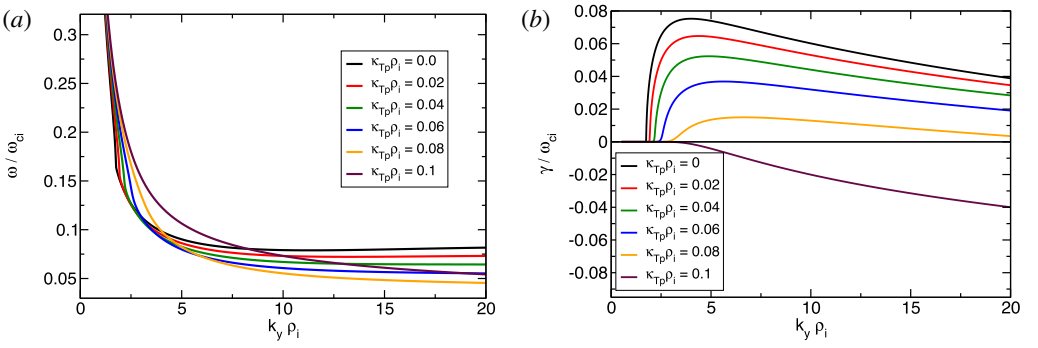

FIGURE 10. Frequency and growth rate of the ETG mode in a pure pair plasma when the symmetry between the species is broken by a difference in the electron and positron temperature profiles. The electron temperature profile with $\kappa_{Te}\rho_i = 0.1$ is kept fixed. Here, $\lambda_D/\rho_i = 0.1$ and $\tau_a = 1$ with $a = (e, p)$. Note that $\rho_i = \sqrt{m_H T_e}/(eB)$ with m_H the proton mass is used here as a normalisation constant since pure pair plasmas do not contain ions.

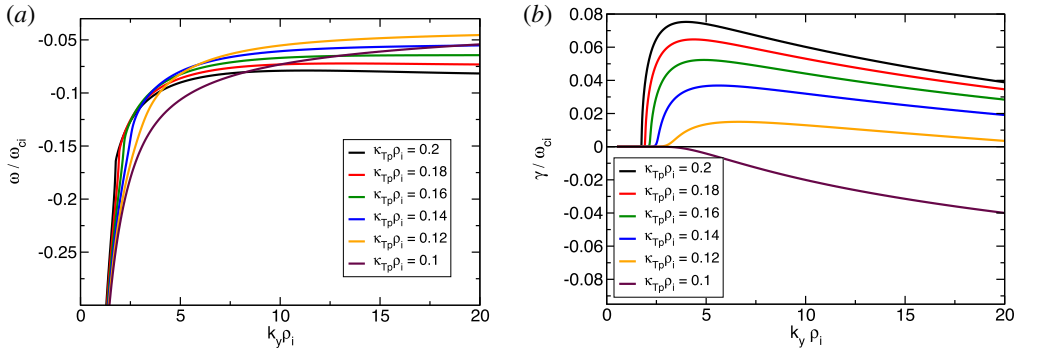

FIGURE 11. Frequency and growth rate of the positron-temperature-gradient mode in a pure pair plasma when the symmetry between the species is broken by a difference in the electron and positron temperature profiles. The electron temperature profile with $\kappa_{Te}\rho_i = 0.1$ is kept fixed. Here, $\lambda_D/\rho_i = 0.1$ and $\tau_a = 1$ with $a = (e, p)$. Note that $\rho_i = \sqrt{m_H T_e}/(eB)$ with m_H the proton mass is used here as a normalisation constant since pure pair plasmas do not contain ions.

7. Shear Alfvén wave

Finally, we consider a homogeneous plasma (all profiles are flat) and solve the electromagnetic dispersion relation (2.15) at finite β. In this case, there are no sources of free energy and, hence, no instabilities (all modes are damped or marginal). From the definition of the plasma dispersion function, equation (2.12), one can derive $Z_{1a} = 1 + \zeta_a Z_{0a}$ and $Z_{2a} = \zeta_a Z_{1a}$. Assuming $k_\parallel v_{thi} \ll \omega \ll k_\parallel v_{the}$, one can thus write:

$$Z_{0i} = -\frac{1}{\zeta_i} - \frac{1}{2\zeta_i^3} + O\left(\frac{1}{\zeta_i^5}\right), \quad Z_{0(e,p)} = \mathrm{i}\sqrt{\pi} + O(\zeta_e) \qquad (7.1a,b)$$

$$Z_{1i} = -\frac{1}{2\zeta_i^2} + O\left(\frac{1}{\zeta_i^4}\right), \quad Z_{1(e,p)} = 1 + O(\zeta_e) \qquad (7.2a,b)$$

https://doi.org/10.1017/S0022377818000181 Published online by Cambridge University Press

$$Z_{2i} = -\frac{1}{2\zeta_i} + O\left(\frac{1}{\zeta_i^3}\right), \quad Z_{2(e,p)} = \zeta_e + O(\zeta_e^2). \tag{7.3a,b}$$

For flat profiles $\omega_{*a} = 0$ and $\eta_a = 0$. Hence, from (2.9)

$$W_{0a} = \zeta_a Z_{0a} \Gamma_{0a}, \quad W_{1a} = \zeta_a Z_{1a} \Gamma_{0a}, \quad W_{2a} = \zeta_a Z_{2a} \Gamma_{0a}. \tag{7.4a–c}$$

We consider perpendicular scales much larger than the electron gyroradius so that one can neglect electron and positron FLR effects, implying $\Gamma_{0e} = 1$ and $\Gamma_{0p} = 1$. Employing the appropriate expansions of the plasma dispersion function, we obtain:

$$W_{0i} = -\Gamma_{0i} - \frac{\Gamma_{0i}}{2\zeta_i^2} + O\left(\frac{1}{\zeta_i^4}\right), \quad W_{0(e,p)} = \mathrm{i}\zeta_{e,p}\sqrt{\pi} + O\left(\zeta_{e,p}^2\right) \tag{7.5a,b}$$

$$W_{1i} = -\frac{\Gamma_{0i}}{2\zeta_i} + O\left(\frac{1}{\zeta_i^3}\right), \quad W_{1(e,p)} = \zeta_{e,p} + O\left(\zeta_{e,p}^2\right) \tag{7.6a,b}$$

$$W_{2i} = -\frac{\Gamma_{0i}}{2} + O\left(\frac{1}{\zeta_i^2}\right), \quad W_{2(e,p)} = \zeta_{e,p}^2 + O\left(\zeta_{e,p}^3\right). \tag{7.7a,b}$$

For equal temperatures and charges of the species, equation (2.15) becomes

$$\left(1 + k_\perp^2 \lambda_D^2 + \frac{1}{2}\sum_a \nu_a W_{0a}\right)\left(1 - \sum_a \frac{2\beta_a}{k_\perp^2 \rho_a^2} W_{2a}\right) + \sum_a \nu_a W_{1a} v_{tha} \sum_a \frac{\beta_a}{k_\perp^2 \rho_a^2} \frac{W_{1a}}{v_{tha}} = 0. \tag{7.8}$$

Here, the notation $\beta_a = \mu_0 n_a T_a / B^2$ is used. Note that the usual assumption of small β_a has been implicitly made in the derivation of the original dispersion relation (2.15) since we have neglected the parallel magnetic field perturbation $\delta B_\parallel$. We substitute the approximate expressions for W_{na}, equations (7.5)–(7.7), into the dispersion relation (7.8). Note that the small terms of the order $1/\zeta_i^2$ and $1/\zeta_i$ must be kept in W_{0i} and W_{1i}, respectively, since they give order-unity contributions in the dispersion relation when multiplied with ζ_e^2 appearing in $W_{2(e,p)}$ and $W_{1(e,p)}^2$. For equal temperatures and charges of the species, implying $\zeta_e = \zeta_p$, one can write:

$$\frac{\zeta_e^2}{\rho_e^2} = \frac{\zeta_i^2}{\rho_i^2}, \quad \zeta_e v_{the} = \zeta_i v_{thi}, \quad \beta_a = \nu_a \beta_e, \quad \nu_i + \nu_p = 1. \tag{7.9a–d}$$

Using these relations and assuming $k_\parallel v_{thi} \ll \omega \ll k_\parallel v_{the}$, one can write the dispersion relation to the lowest order as follows:

$$\left(1 + k_\perp^2 \lambda_D^2 - \frac{\nu_i \Gamma_{0i}}{2}\right)\left[1 - \frac{2\beta_e \zeta_e^2 (1+\nu_p)}{k_\perp^2 \rho_e^2}\right] + (1+\nu_p)^2 \frac{\beta_e \zeta_e^2}{k_\perp^2 \rho_e^2} + \frac{\nu_i \beta_e \Gamma_{0i}}{k_\perp^2 \rho_i^2}\left[\frac{\nu_i}{2}(1-\Gamma_{0i}) + k_\perp^2 \lambda_D^2\right] = 0. \tag{7.10}$$

https://doi.org/10.1017/S0022377818000181 Published online by Cambridge University Press

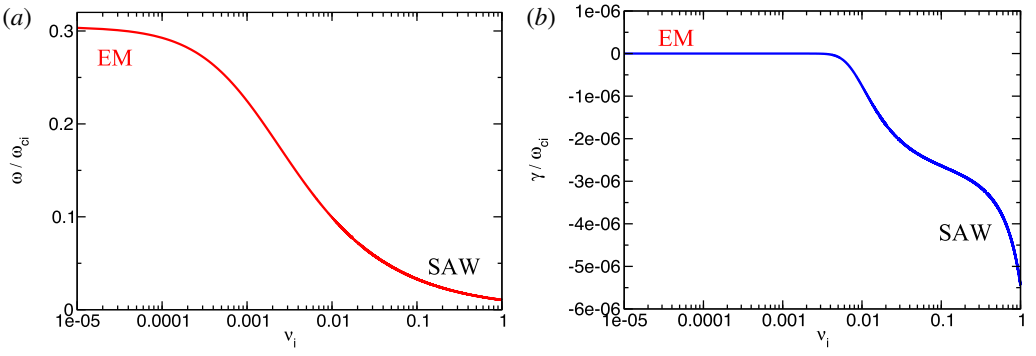

FIGURE 12. Frequency and growth rate of the shear Alfvén wave (SAW) as a function of ion contamination in a pair plasma for $k_\perp \rho_i = 0.05$, $k_\parallel \rho_i = 7.4 \times 10^{-4}$, $\lambda_D/\rho_i = 0.01$ and $\beta_e = 0.005$. One sees the transition from the SAW regime $\nu_i \sim 1$ to a regime of an electromagnetic wave travelling at the speed of light when $\nu_i \to 0$. The latter limit is not properly described by the gyrokinetic theory of this paper since the relativistic effects must be taken into account in the wave dynamics (Zocco 2017).

For conventional plasmas with $\nu_i = 1$ and $\nu_p = 0$, with the long-wavelength approximation $\Gamma_{0i} \approx 1 - k_\perp^2 \rho_i^2$, valid at small $k_\perp \rho_i < 1$, and for $k_\perp \lambda_D \to 0$, this dispersion relation reduces to the shear Alfvén wave (SAW):

$$2\beta_e \zeta_i^2 = 1 \quad \Leftrightarrow \quad \omega^2 = k_\parallel^2 \frac{B^2}{\mu_0 m_i n_{0e}} = k_\parallel^2 v_A^2 \equiv \omega_A^2. \tag{7.11}$$

For a finite positron fraction, one can write

$$2\beta_e \zeta_i^2 = \frac{1}{\nu_i} \frac{2 - \nu_i \Gamma_{0i} + O(\beta_e)}{2 - \nu_i} \frac{k_\perp^2 \rho_i^2}{1 - \Gamma_{0i}} \tag{7.12}$$

if the Debye length is neglected. In the long-wavelength approximation $\Gamma_{0i} \approx 1 - k_\perp^2 \rho_i^2$

$$2\beta_e \zeta_i^2 = \frac{1}{\nu_i} \quad \Leftrightarrow \quad \omega = \omega_A / \sqrt{\nu_i} = k_\parallel \frac{B}{\sqrt{\mu_0 m_i n_{0i}}} = k_\parallel^2 v_{Ai}^2 \equiv \omega_{Ai}. \tag{7.13}$$

The numerical solution of the full dispersion relation (2.15) for the shear Alfvén wave parameters is shown in figure 12. One sees, as expected, that the frequency of the shear Alfvén wave increases very rapidly when $\nu_i \to 0$ (note the logarithmic scale in the figure), in agreement with our findings and Helander & Connor (2016). For $\nu_i = 1$, the classic shear Alfvén wave is recovered, see (7.11).

Note that (7.13) highlights the role of the ions, which carry most of the plasma inertia even at small ν_i, but it is singular for $\nu_i = 0$. This formal singularity can be resolved taking the finite Debye length into account. In the long-wavelength approximation ($\Gamma_{0i} \approx 1 - k_\perp^2 \rho_i^2$ valid for $k_\perp \rho_i < 1$), one obtains:

$$2\beta_e \zeta_i^2 = \frac{2 - \nu_i + 2k_\perp^2 \lambda_D^2}{\nu_i k_\perp^2 \rho_i^2 + 2k_\perp^2 \lambda_D^2} \frac{k_\perp^2 \rho_i^2}{2 - \nu_i} = \frac{1}{\nu_i + 2\lambda_D^2/\rho_i^2} \left[1 + O\left(k_\perp^2 \lambda_D^2\right)\right]. \tag{7.14}$$

https://doi.org/10.1017/S0022377818000181 Published online by Cambridge University Press

This equation describes coupling of the 'ion shear Alfvén wave', based on ion inertia, to a wave travelling at the speed of light (Zocco 2017). Indeed, in a pure pair plasma, the dispersion relation (7.14) reduces for small $k_\perp \lambda_D < 1$ to

$$\omega^2 = k_\parallel^2 \frac{B^2}{\mu_0 m_e n_{0e}} \frac{\rho_e^2}{2\lambda_D^2} \quad \Leftrightarrow \quad \omega = k_\parallel c. \tag{7.15}$$

As shown in figure 12, the SAW transforms for $\nu_i \to 0$ into the electromagnetic wave. The displacement current, not included into the original dispersion relation (2.15), must be taken into account for this wave in order to address it properly, see (Zocco 2017) for details. Recall that we have assumed $\omega \ll k_\parallel v_{\mathrm{the}}$ in our derivation of (7.10). Then, the solution $\omega = k_\parallel c$ implies $c \ll v_{\mathrm{the}}$ which physically cannot be true. Therefore, equation (7.15) is just a formal limit to which the SAW solution reduces at $\nu_i \to 0$ and small, but finite, $k_\perp \lambda_D$. Note that one can still satisfy the gyrokinetic ordering $\omega \ll \omega_{ce}$ for this formal limit, $\omega = k_\parallel c$, if $k_\parallel \rho_e \ll v_{\mathrm{the}}/c$.

For large $k_\perp \lambda_D > 1$ and $\lambda_D > \rho_i$, the long-wavelength approximation cannot be used. The dispersion relation appropriate for this case is

$$2\beta_e \zeta_i^2 = \frac{2 - \nu_i \Gamma_{0i} + 2k_\perp^2 \lambda_D^2}{\nu_i (1 - \Gamma_{0i}) + 2k_\perp^2 \lambda_D^2} \frac{k_\perp^2 \rho_i^2}{2 - \nu_i}. \tag{7.16}$$

For $k_\perp \lambda_D \gg 1$, a solution with $\omega \sim k^2$ can be obtained (recall that $0 \leqslant \Gamma_{0i} \leqslant 1$):

$$2\beta_e \zeta_e^2 = \frac{k_\perp^2 \rho_e^2}{2 - \nu_i} \quad \Leftrightarrow \quad \omega = \frac{1}{2 - \nu_i} \frac{k_\perp \rho_e}{\sqrt{\beta_e}} k_\parallel v_{\mathrm{the}}. \tag{7.17}$$

A solution of this kind can be found in conventional plasmas, in proton-contaminated pair plasmas, and in pure pair plasmas as shown in figure 13, where the dispersion relation (2.15) is solved numerically. The transitions between the shear Alfvén wave, electromagnetic wave and the $\omega \sim k^2$ solution can be seen clearly. Note that the quadratic dispersion relation (7.17) is formally similar to the whistler wave although its physics must be different since the Hall effect is absent in pure pair plasmas.

8. Conclusions

In this paper, we have studied the gyrokinetic stability of pair plasmas solving the dispersion relation (2.15) analytically and numerically. It is found that pair plasmas can support the gyrokinetic ITG, ETG and universal instabilities even in slab geometry if the proton fraction exceeds some threshold. In practice, however, this threshold is usually quite large, hopefully large enough to keep the proton content below this value in pair-plasma experiments (Pedersen *et al.* 2012). These results extend the finding of Helander (2014) that pair plasmas are stable to gyrokinetic modes in the absence of magnetic curvature to the cases with small to moderate proton contamination. We find, however, that pure pair plasmas can have temperature-gradient-driven instabilities, if the electron and the positron temperature profiles differ. In reality, however, such profiles are unlikely in steady state, since the characteristic time of energy exchange between the species is comparable to the Maxwellisation time. In the electromagnetic regime, we find that the shear Alfvén wave is present in a contaminated plasma. Its frequency increases very rapidly when the ion fraction becomes negligible.

https://doi.org/10.1017/S0022377818000181 Published online by Cambridge University Press

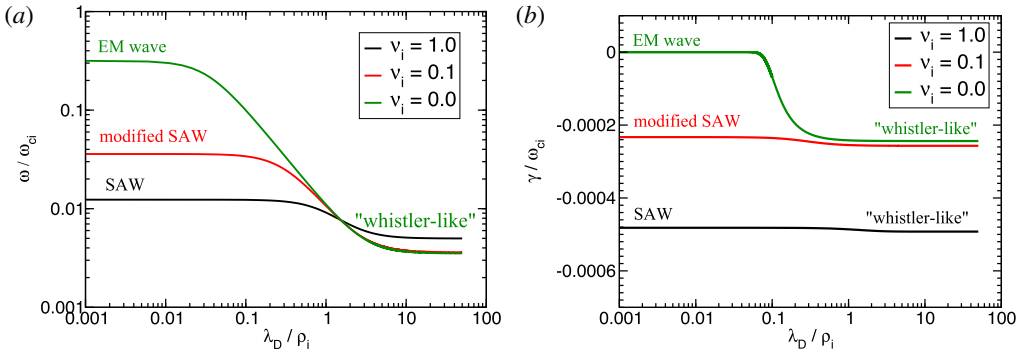

FIGURE 13. Frequency and growth rate of the shear Alfvén wave (SAW), 'whistler-like' and electromagnetic (EM) wave as a function of the Debye length in a conventional plasma, proton-contaminated pair plasma and pure pair plasma. Transitions between different regimes are clearly seen. The parameters used are $k_\perp \rho_i = 0.475$, $k_\parallel \rho_i = 7.4 \times 10^{-4}$ and $\beta_e = 0.005$. Note that $\lambda_D \gtrsim \rho_e/\sqrt{\beta_e}$ implies $v_{\mathrm{the}} \gtrsim c$. The physics of this case is not properly described by the gyrokinetic theory of this paper since relativistic effects must be taken into account in the particle dynamics and distribution functions (Zocco 2017). The 'whistler-like' solution is a formal limit of the SAW dispersion relation at large $k_\perp \lambda_D$.

Acknowledgements

We acknowledge T. S. Pedersen and PAX/APEX experiment team for their interest to our work. A.M. thanks V. S. Mikhailenko and V. D. Yegorenkov for bringing his attention to the K-mode solutions of kinetic dispersion relations. R. Kleiber is acknowledged for providing a module for a numerical root finding.

REFERENCES

CARPENTIER, M. P. & SANTOS, A. F. D. 1982 Solution of equations involving analytic functions. *J. Comput. Phys.* **45**, 210–220.

COPPI, B., ROSENBLUTH, M. N. & SAGDEEV, R. Z. 1967 Instabilities due to temperature gradients in complex magnetic field configurations. *Phys. Fluids* **10**, 582–587.

DAVIES, B. 1986 Locating the zeros of an analytic function. *J. Comput. Phys.* **66**, 36–49.

FRIED, B. D. & GOULD, R. W. 1961 Longitudinal ion oscillations in a hot plasma. *Phys. Fluids* **4** (1), 139–147.

HELANDER, P. 2014 Microinstability of magnetically confined electron–positron plasmas. *Phys. Rev. Lett.* **113**, 135003+4.

HELANDER, P. & CONNOR, J. W. 2016 Gyrokinetic stability theory of electron–positron plasmas. *J. Plasma Phys.* **82**, 9058203+13.

PEDERSEN, T., BOOZER, A. H., DORLAND, W., KREMER, J. P. & SCHMITT, R. 2003 Prospects for the creation of positron–electron plasmas in a non-neutral stellarator. *J. Phys B: At. Mol. Opt. Phys.* **36**, 1029–1039.

PEDERSEN, T. S., DANIELSON, J. R., HUGENSCHMIDT, C., MARX, G., SARASOLA, X., SCHAUER, F., SCHWEIKHARD, L., SURKO, C. M. & WINKLER, E. 2012 Plans for the creation and studies of electron–positron plasmas in a stellarator. *New J. Phys.* **14**, 03510+13.

SAITOH, H., STANJA, J., STENSON, E. V., HERGENHAHN, U., NIEMANN, H., PEDERSEN, T.S., STONEKING, M.R., PIOCHACZ, C. & HUGENSCHMIDT, C. 2015 Efficient injection of an intense positron beam into a dipole magnetic field. *New J. Phys.* **17**, 103038+9.

https://doi.org/10.1017/S0022377818000181 Published online by Cambridge University Press

YEGORENKOV, V. & STEPANOV, K. 1987 Kinetychni potenzialni elektronni hvyli u plasmi. *Dop. Akademii Nauk URSR, Ser.* A (8), 44.

YEGORENKOV, V. & STEPANOV, K. 1988 Electron cyclotron k-modes in plasmas. *J. Expl Theor. Phys.* **94**, 116.

ZOCCO, A. 2017 Slab magnetised non-relativistic low-beta electron–positron plasmas: collisionless heating, linear waves and reconnecting instabilities. *J. Plasma Phys.* **83**, 715830602+17.